A R C H I V E S O F M E T A L L U R G Y A N D M A T E R I A L S
Volume 60 2015 Issue 2
DOI: 10.1515/amm-2015-0222

I. KALEMBA*,♯, M. KOPYŚCIAŃSKI*, C. HAMILTON**, S. DYMEK*

NATURAL AGING BEHAVIOR OF FRICTION STIR WELDED Al-Zn-Mg-Cu ALUMINUM ALLOYS

STARZENIE NATURALNE ZŁĄCZY STOPÓW ALUMINIUM Al-Zn-Mg-Cu WYKONANYCH METODĄ ZGRZEWANIA TARCIOWEGO Z MIESZANIEM MATERIAŁU

The long term natural aging behavior of friction stir welded aluminum 7136-T76 and 7042 T6 extrusions was investigated. The microstructural characteristics and mechanical properties in the as-welded and six years naturally aged conditions were studied and correlated to a coupled thermal/material flow model of the joining process. Hardness profiles for the 7136 alloy taken along the mid-plane thickness of the workpiece displayed the characteristic W-shape. With natural aging, hardness recovery occurred on both sides of the weld, but the position of the hardness minima, particularly on the advancing side, shifted away from the weld centerline. The hardness profile for the 7042 alloy displayed U-shape in the as-welded condition and W-shape after natural aging. The hardness behavior upon natural aging correlated to the temperature profile developed during welding and the degree to which phase dissolution occurred in the regions adjacent to the stir zone.

Keywords: Friction stir welding, Natural aging, Aluminum alloys, Thermal analysis

W artykule przedstawiono wyniki badań dotyczące długoterminowego starzenia naturalnego złączy stopów aluminium 7136-T76 i 7042-T6 wykonanych metodą zgrzewania tarciowego z mieszaniem materiału. Złącza w stanie po zgrzewaniu oraz po 6 latach starzenia naturalnego scharakteryzowano pod względem mikrostrukturalnym oraz mechanicznym. Wyniki badań skorelowano z modelem termicznym i modelem płynięcia materiału podczas zgrzewania. Profil twardości złącza stopu 7136 wykazuje charakterystyczny kształt litery „W". Starzenie naturalne powoduje wzrost twardości, przy czym minimum twardości, szczególnie po stronie natarcia, odsuwa się od środka złącza. Profil twardości złącza stopu 7042 przyjmuje kształt litery „U" po zgrzewaniu i kształt litery „W" po starzeniu naturalnym. Takie zachowanie twardości po starzeniu naturalnym jest związane z temperaturą podczas procesu zgrzewania oraz stopniem, w jakim rozpuszczają się fazy w obszarach sąsiadujących ze strefą mieszania.

1. Introduction

Friction stir welding (FSW) is already a well-established technique that is particularly suitable for joining high strength Al-Zn-Mg-Cu aluminum alloys (7000 series). These alloys are regarded as non-weldable by traditional fusion welding. However, FSW is a method that occurs in solid state and overcomes all disadvantages associated with material melting and subsequent crystallization. That is why this technology has experienced growing popularity in the manufacture of ships, airplanes, cars, railway carriages etc. where high strength aluminum alloys are commonly employed. Though FSW basics have been previously described in a few review papers, e.g. [1-5], some issues regarding the process-microstructure-properties relationship remain unclear and require further research. Even though it has been already found that high-quality, sound welds with good mechanical properties may be produced between non-weldable aluminum alloys of the 7000 series [6,7], the phenomena occurring spontaneously after welding (natural aging) in these alloys need further explanation. Some papers discussed this issue [8-12], however, the differences in the course of natural aging in particular alloy weldments call for additional research that provide more evidence for deeper understanding of this apparently simple phenomenon. This study concentrated on the long-term effect of natural aging (up to six years) in friction stir welds of 7136 and 7042 aluminum alloys. The primary objective was to compare the changes induced by natural aging in the hardness profiles across friction stir welds of these alloys.

2. Materials and experimental procedures

The present study focuses on the hardness changes in friction stir welds of two Al-Zn-Mg-Cu aluminum alloys subjected to long term natural aging. The experiments were conducted on 7136 and 7042 alloys. The alloys belong to the most advanced class of precipitation strengthened aluminum alloys. Their chemical compositions are similar, but one of them, (7042), additionally contains scandium. The chemical

* AGH UNIVERSITY OF SCIENCE AND TECHNOLOGY, AL. A. MICKIEWICZA 30, 30-059 KRAKÓW, POLAND
** MIAMI UNIVERSITY, OXFORD, OHIO, USA
♯ Corresponding author: kalemba@agh.edu.pl

compositions of the investigated alloys are given in TABLE 1. Both alloys were cast by direct chill technology, extruded as 6.35 mm thick bars and then heat treated. The alloy 7136 was treated to the T76 temper and the 7042 to the T6 temper.

TABLE 1
Content of principal elements in examined alloys

Element [wt.%]	7136 alloy	7042 alloy
Zn	7.94	6.89
Mg	1.99	2.38
Cu	1.93	1.45
Zr	0.14	0.14
Sc	-	0.25
Al	Balance	Balance

The blanks of these alloys were friction stir welded in a butt joint configuration along the extrusion longitudinal direction by the Edison Welding Institute (EWI) in Columbus, Ohio, USA. The joining was performed with the same welding velocity – 2.1 mm/s but different tool rotation speed – 250 revolutions per minute (RPM) for 7136 and 175 RPM for 7042. Also the applied force was different: 26.7 kN for 7136 and 24.7 kN for 7042. The diameter of the FSW tool shoulder was 17.8 mm, the pin diameter tapered linearly from 10.3 mm at the tool shoulder to 7.7 mm at the tip and the pin depth was 6.1 mm. More specific details of the tool design are proprietary to EWI.

The hardness tests were performed on a Tukon 2500 hardness tester using a 9.81 N load for 10 seconds. The hardness was measured at the mid-thickness of the transverse plane of the joint. The distance between sampling points was 1 mm.

Microstructure of the welds was examined on sections perpendicular to the weld direction. Light microscopy (LM) using polarizing light as well as transmission electron microscopy (TEM) were used for this purpose. The polished samples for LM were anodized in an electrolyte containing 1.8 ml HBF_4 and 100 ml water. For TEM examination thin foils were excised from the stirred zone. The samples were electropolished in a solution of nitric acid/methanol (1:2) at -30°C. The utilized voltage was 12 V.

For thermal analysis, small samples were cut out from the parent material as well as from the stir zone of naturally aged weldments. The samples were sealed in aluminum pans and analyzed in a DuPont 910 differential scanning calorimeter using an inert atmosphere. Samples were heated from room temperature at a constant heating rate of 20°C/min.

3. Results and Discussion

The detailed characterization of the microstructure in particular zones in the examined alloys was addressed in earlier papers by the authors' [6,7,13-15]. Despite the microstructural differences of the parent materials, the weld microstructures of the 7136 and 7042 alloys observed in light microscopy scale appear very similar. The macroscopic views of tested joints are presented in Fig. 1. Both microstructures are composed of the zones typical to FSW microstructures: the stirred zone (SZ), thermomechanically affected zone (TMAZ) and heat affected zone (HAZ). The welds were free from defects, however, well defined inhomogeneities referred to in the literature as "onion rings" were revealed in polarized light. The "onion rings" in the 7042 alloy were more distinct. A possible explanation for the formation of "onion rings" in the 7042 alloy was addressed in the authors' earlier paper [16].

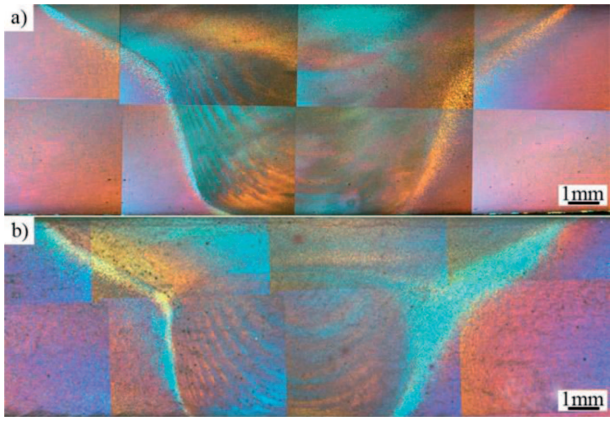

Fig. 1. Optical macrograph of the weld regions: a) 7136 alloy, b) 7042 alloy

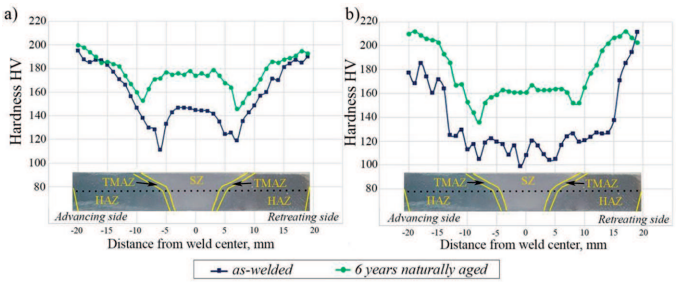

Fig. 2. Microhardness distributions of FSW joints for as-welded and naturally aged conditions: a) 7136 alloy, b) 7042 alloy

The hardness of the 7136 and 7042 alloys in the as-received condition was similar and averages approximately 200 HV. Hardness profiles after welding and natural aging of the tested joints are shown in Fig. 2. The profiles demonstrate the variation in hardness between the particular weld zones and also highlight their responses to natural aging. As observed in FSW welds of other aluminum alloys, the shape of the hardness profile of the 7136 as-welded sample (measured as close to post-welding as practically permissible) consists of a region of higher hardness in the center (nugget), but significantly less than the hardness of the parent metal, surrounded by regions of lower hardness values (Fig. 2a). Thus, the profile exhibits the shape typical for FSW welds of heat treatable aluminum alloys [4] showing a hardness plateau in the central part of the weld (SZ) and two minima on either side of this plateau coinciding with the transition between the TMAZ and HAZ (W-shaped profile). The hardness minima lay within regions of the weld that experienced process temperatures in the range of 280 to 340°C, according to the numerical model elaborated in our previous research [12]. The hardness of the stir zone region (nugget) was less than that of the base material in the T76 temper, even after 6 years of natural aging. After natural aging for 6 years, the hardness profiles still retained the

W-shape, but the hardness magnitudes within the weld zones increased.

The numerical model of temperature distribution during welding of the 7136 alloy, presented and discussed in Ref. [12], clearly demonstrates that the temperature profile is asymmetrical and that higher welding temperatures are achieved on the advancing side with the highest temperature (340°C) occurring approximately 5.25 mm from the tool center. As the tool advances during welding, cooler material in front of the tool is introduced at the leading edge and then swept to the retreating side. As the material is processed by the tool, heated material flows toward the trailing edge and then either deposits toward the advancing side or flows into the workpiece thickness. This flow of material effectively raises the advancing side temperature above that of the retreating side. The numerical model was also adapted for the welding of the 7042 alloy, and the temperature distribution followed the same asymmetry as 7136 with the maximum temperature occurring on the advancing side toward the leading edge at a distance of 4.82 mm from the tool center. However, the maximum temperature for 7042 (and the welding temperatures in general) was less than that observed for 7136. The maximum temperature during welding of 7042 was 286°C, compared to 340°C for 7136.

The post-weld hardness profiles correlate to the process temperatures relative to the precipitate formation and/or precipitate dissolution temperatures of the alloys. For example, as discussed in Ref. [12], the dissolution of stable phases occurs when the welding temperature is greater than the dissolution temperature. However, due to the asymmetric temperature profile in the workpieces during welding, the extent of equilibrium phase dissolution will be different on the retreating and advancing sides. Since the temperature profile is skewed toward the advancing side in the 7136 alloy the dissolution occurs to a greater distance from the weld centerline on the advancing side than on the retreating side. Therefore, equilibrium phases dissolve to a greater extent on the advancing side than on the retreating side. To that end, Figures 3 and 4 display DSC traces of the samples naturally aged for 6 years excised from the stir zones of friction stir welded 7136 and 7042 respectively. The course of the heat flow curves for both alloys is similar but not identical. The significant difference is that the exothermic peak spans a larger temperature range in the 7042 alloy (actually there are two overlapping peaks) than in 7136 and that the exothermic peak is not followed by the deep endothermic peak. This indicates that dissolution of stable η and T phases in 7042 is pronouncedly retarded.

For 7136, therefore, the welding temperatures place the microstructure well within the endothermic peak shown in Fig. 3, indicating that dissolution of η and T phases occurs during processing. The degree of dissolution directly impacts the hardness of the as-welded condition and the hardness of the naturally-aged conditions. After welding, since more complete dissolution occurs on the advancing side outside of the stir zone (due to higher temperature), the hardness will be lower on the advancing side than on the retreating side, in agreement with the hardness profiles in Fig. 2a. Also, it was shown for the 7136 alloy [12], that the lowest hardness immediately after welding should correspond with the position of the largest deviation from the dissolution temperature just outside the stir zone on both sides of the weld. However, the higher the difference between the process temperature and the precipitates' dissolution temperature, the larger the driving force for re-precipitation as the welded workpieces naturally age. Therefore, the position of the minimum hardness will follow the temperature profile as the naturally aging time increases. On the advancing side, the position of the hardness minimum shifts with naturally aging from just adjacent to the stir zone up to 9 mm from the weld centerline and on the retreating side, the position of the hardness minimum shifts up to 7 mm from the weld centerline. As shown in Fig. 2a, the position of the minimum hardness on the advancing side begins at 6 mm in the as-welded condition, but moves to 9 mm after six years of natural aging. On the retreating side, the position of the hardness minimum in the as-welded condition appears at 7 mm from the weld centerline, and it remained in this position with natural aging up to six years. Similar displacements in the hardness minima as a function of natural aging time were previously reported by Leonard [8] in friction stir welded aluminum alloys 2014A-T651 and 7075-T651, however, the author did not elaborate on the origin of these displacements in the discussion of the results. This same behavior in the hardness profiles can also be observed in graphs presented by Fuller et al. [10] in their research on friction stir welded aluminum 7050 and 7075, but again, the authors did not discuss the phenomenon. Also, the review paper by Threadgill et al. [2] displays hardness profiles for naturally aged FSW weld in 7075-T6 alloy in which the positions of the minima clearly change with aging time, but the phenomenon is not addressed in the article.

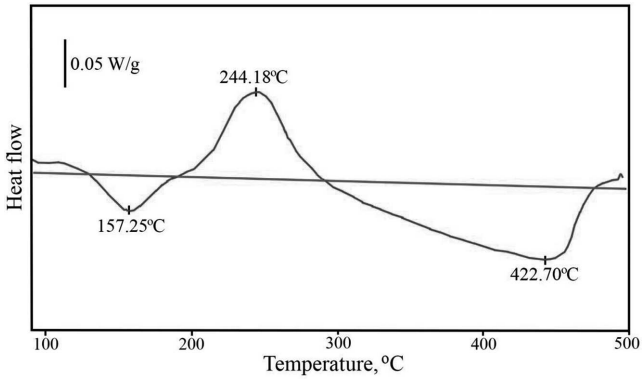

Fig. 3. Differential scanning calorimetry trace of the stir zone in the 7136 alloy naturally aged for six years

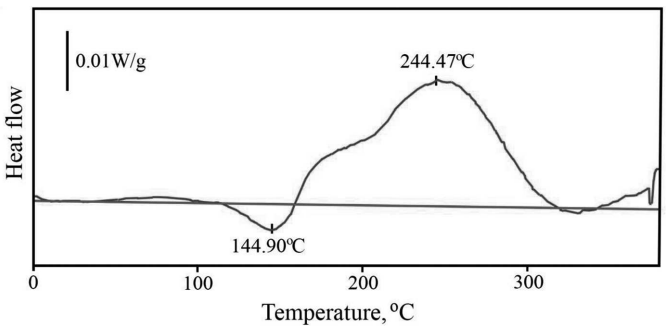

Fig. 4. Differential scanning calorimetry trace of the stir zone in the 7042 alloy naturally aged for six years

The strengthening precipitates that went into solution during welding will re-precipitate upon cooling and natural aging. Those precipitates that did not dissolve during welding, however, will have coarsened and remained stable within the microstructure post-welding. This results in a bi-modal particle size distribution in the as-welded condition. The size of coarser precipitates in the 7136 alloy was in the range of 50-150 nm, with larger particles located on grain and subgrain boundaries, while the finer precipitates exhibited a size of about 10 nm (Fig. 5a). In addition, some residual dislocations were often observed as a result of incomplete recrystallization.

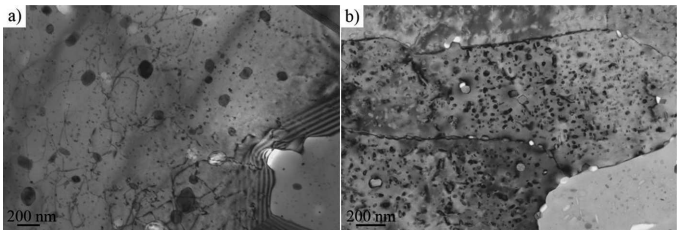

Fig. 5. Typical microstructures of the stir zones in TEM scale: a) 7136 alloy, b) 7042 alloy

For 7042, on the other hand, the lower welding temperatures place the microstructure in proximity to the exothermic peak shown in Figure 4, indicating that precipitation and coarsening of η and T phases occur during welding. In general, the retreating side temperatures are below the peak position, and the advancing side temperatures are above the peak position. Both, the retreating side and advancing sides are characterized by η and T phases that precipitate and primarily coarsen during welding, however the coarsening on the advancing side is more intense than on the retreating side due to higher welding temperature. Therefore, the concentration of solutes in the solid solution should be higher on the retreating side giving rise to higher driving force for further hardness rcovery. As a result, greater hardness recovery occurs on the retreating side during natural aging of the 7042 alloy than on the advancing side as shown in Fig. 2b. The TEM image of naturally aged 7042 in Fig. 5b demonstrates that the volume fraction of particles is much greater than that observed for 7136, confirming that coarsening rather than dissolution took place during welding giving rise to lower hardness and smaller driving force for nucleation of GP zones during natural aging.

The hardness profile for the 7042 alloy weldments also exhibited a different shape in the as-welded condition. It is U-shaped rather than W-shaped and the hardness plateau extends over a larger distance than in the 7136 weldments (Fig. 2b). The fluctuations of hardness values at the plateau are likely associated with the presence of "onion rings" since, as was discussed in Ref. [16], "onion rings" are composed of the particle-rich and particle-poor bands. However, the 6 years natural aging altered the shape of hardness profile to become W-shaped, which is typical to age hardenable aluminum alloys. The hardness minima on this profile are in similar positions as the 7136 weldment, however, the minimum on the advancing side is deeper than on the retreating one. It is also interesting that the hardness in the weld center in the 7042 alloy is lower than the corresponding value in the 7136 alloy despite the fact that the hardness values about 20 mm away from the weld center are comparable in both alloys. This indicates that the re-precipitation of strengthening phases in the 7042 alloys is much slower than in the 7136 alloy. Such a behavior may be explained by the combined effect of the presence of scandium in the chemical composition as well as less severe welding conditions – lower rotational speed and smaller force results in lower heat input during the welding process. Also, it was already well documented that the addition of scandium decreases the diffusion rate of alloying additions in aluminum [17].

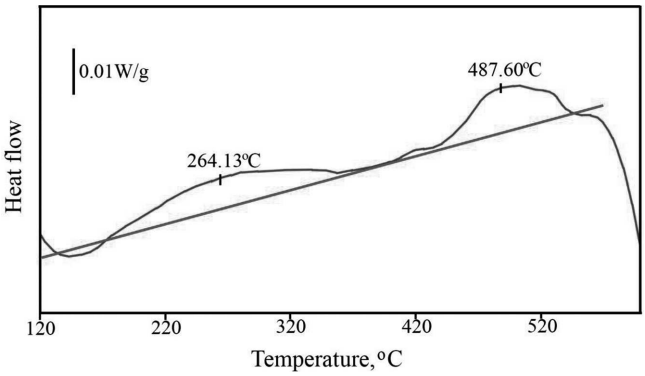

Fig. 6. Differential scanning calorimetry thermogram for the parent 7042 alloy

The consequence of this effect in the 7042 alloy is that coarsening of the strengthening phases prevails over their dissolution during the welding process. This is confirmed by the DSC thermogram of the parent 7042 alloy sample (Fig. 6) that shows only a small endothermic peak corresponding to the limited dissolution of the GP zones. Also, transmission electron microscopy revealed a high density of relatively coarse particles in the 7042 stir zone, contrary to the microstructure found in the stir zone of the 7136 alloy (Fig. 5). For this reason, the re-precipitation of GP zones during natural aging is strongly retarded giving a broad hardness plateau in the as-welded condition and a much weaker natural aging response after 6 years. Assuming that the temperature distribution during FSW of the 7042 alloy was qualitatively the same as for the 7136 alloy, the 6-year hardness profile for the 7042 alloy corresponds in-character to the as-welded profile for the 7136 alloy. This means that long term natural aging of the 7042 weldments is equivalent to the aging that occurs just after welding in the 7136 alloy.

4. Conclusions

In this study, the effect of natural aging on the mechanical properties of friction stir welded 7136 and 7042 aluminum alloys has been analyzed. The following important conclusions have been drawn:

1. There is a substantial difference in hardness profiles between 7136 and 7042 alloys that influence the behavior of these alloys during natural aging.
2. The W-shaped hardness profile occurs for the 7136 alloy while the 7042 alloy exhibits U-shaped profile.
3. The hardness recovery is faster in the 7136 alloy.

Acknowledgements

The authors acknowledge the AGH University of Science and Technology for the support of this research within the Project No. 11.11.110.295.

REFERENCES

[1] R.S. Mishra, M.W. Mahoney, Friction Stir Welding and Processing, ASM International, USA 2007.
[2] P.L. Threadgill, A.J. Leonard, H.R. Sherliff, P.J. Withers, Int Mater Rev. **54**, 49 (2009).
[3] M.B. Uday, M.N. Ahmad Fauzi, H. Zuhailawati, A.B. Ismail, Sci Technol Weld Joi. **15**, 534 (2010).
[4] R.S. Mishra, Z.Y. Ma, Mater Sci Eng. **50**, 1 (2005).
[5] R. Nandan, T. DebRoy, H.K.D.H. Bhadeshia. Prog Mater Sci. **53**, 980 (2008).
[6] I. Kalemba, M. Kopyscianski, S. Dymek, C. Hamilton, Steel Res Int. **81**, 1088 (2010).
[7] I. Kalemba, S. Dymek, C. Hamilton, M. Blicharski, Mater Sci Tech. **27**, 903 (2011).
[8] A.J. Leonard. Proceedings of 2nd International Symposium on FSW; Götheborg (2000).
[9] T.W. Nelson, R.J. Steel, W.J. Arbegast, Sci Technol Weld Joi. **8**, 283 (2003).
[10] C.B. Fuller, M.W. Mahoney, M. Calabrese, L. Micona, Mat Sci Eng A. **527**, 2233 (2010).
[11] P. Dong, D. Sun, H. Li, Mat Sci Eng A. **576**, 29 (2013).
[12] I. Kalemba, C. Hamilton, S. Dymek, Mater Design. **60**, 295 (2014).
[13] C. Hamilton, S. Dymek, M. Blicharski. Arch Metall Mater. **53**, 1047 (2008).
[14] C. Hamilton, S. Dymek, I. Kalemba, M. Blicharski, Sci Technol Weld Joi. **13**, 714 (2008).
[15] I. Kalemba, S. Dymek, C. Hamilton, M. Blicharski, Arch Metall Mater. **54**, 75 (2009).
[16] C. Hamilton, M. Kopyściański, O. Senkov, S. Dymek, Metall Mater Trans A. **44A**, 1730 (2013).
[17] J. Røyset, N. Ryum, Int Mater Rev. **50**, 19 (2005).

Received: 20 February 2014.